Emphysematous and Nonemphysematous Gas Trapping in Chronic Obstructive Pulmonary Disease: Quantitative CT Findings and Pulmonary Function[1]

Mariaelena Occhipinti, MD
Matteo Paoletti, PhD
Francesca Bigazzi, MD
Gianna Camiciottoli, MD
Riccardo Inchingolo, MD
Anna Rita Larici, MD
Massimo Pistolesi, MD, PhD

Purpose: To identify a prevalent computed tomography (CT) subtype in patients with chronic obstructive pulmonary disease (COPD) by separating emphysematous from nonemphysematous contributions to total gas trapping and to attempt to predict and grade the emphysematous gas trapping by using clinical and functional data.

Materials and Methods: Two-hundred and two consecutive eligible patients (159 men and 43 women; mean age, 70 years [age range, 41–85 years]) were prospectively studied. Pulmonary function and CT data were acquired by pulmonologists and radiologists. Noncontrast agent–enhanced thoracic CT scans were acquired at full inspiration and expiration, and were quantitatively analyzed by using two software programs. CT parameters were set as follows: 120 kVp; 200 mAs; rotation time, 0.5 second; pitch, 1.1; section thickness, 0.75 mm; and reconstruction kernels, b31f and b70f. Gas trapping obtained by difference of inspiratory and expiratory CT density thresholds (percentage area with CT attenuation values less than –950 HU at inspiration and percentage area with CT attenuation values less than –856 HU at expiration) was compared with that obtained by coregistration analysis. A logistic regression model on the basis of anthropometric and functional data was cross-validated and trained to classify patients with COPD according to the relative contribution of emphysema to total gas trapping, as assessed at CT.

Results: Gas trapping obtained by difference of inspiratory and expiratory CT density thresholds was highly correlated ($r = 0.99$) with that obtained by coregistration analysis. Four groups of patients were distinguished according to the prevalent CT subtype: prevalent emphysematous gas trapping, prevalent functional gas trapping, mixed severe, and mixed mild. The predictive model included predicted forced expiratory volume in 1 second/vital capacity, percentage of predicted forced expiratory volume in 1 second, percentage of diffusing capacity for carbon monoxide, and body mass index as emphysema regressors at CT, with 81% overall accuracy in classifying patients according to its extent.

Conclusion: The relative contribution of emphysematous and nonemphysematous gas trapping obtained by coregistration of inspiratory and expiratory CT scanning can be determined accurately by difference of CT inspiratory and expiratory density thresholds. CT extent of emphysema can be predicted with accuracy suitable for clinical purposes by pulmonary function data and body mass index.

Online supplemental material is available for this article.

[1] From the Section of Respiratory Medicine, Department of Experimental and Clinical Medicine, University of Florence, Careggi University Hospital, Largo A. Brambilla 3, 50134 Florence, Italy (M.O., M. Paoletti, F.B., G.C., M. Pistolesi); and Departments of Pulmonology (R.I.) and Radiological Sciences (A.R.L.), Gemelli University Hospital, Catholic University of the Sacred Heart, Rome, Italy. Received July 20, 2017; revision requested September 25; revision received October 9; accepted October 27; final version accepted November 3. **Address correspondence to** M.O. (e-mail: *mariaelena.occhipinti@unifi.it*).

Supported by the Ministry of Health of Italy and Ministry of University and Research of Italy.

The wide heterogeneity of clinical presentation makes chronic obstructive pulmonary disease (COPD) a complex disease that deserves deeper insights beyond airflow obstruction detected at spirometry. The advent of computed tomography (CT) has brought in the last 20 years substantial progress in the assessment of the pathophysiologic mechanisms that underlie airflow obstruction in COPD, namely emphysema and conductive airway disease (1). However, the possibility to accurately resolve at CT the relative contribution of emphysematous and nonemphysematous gas trapping in the determination of expiratory airflow obstruction is still matter of study, to our knowledge (2). Recently, Galbán et al (3) proposed a method called pulmonary parametric response map, which is based on the coregistration of paired inspiratory and expiratory thoracic CT scans. This method can dissect and display the regional distribution of the persistent low density area (emphysematous gas trapping because of parenchymal destruction), and the functional low density area (nonemphysematous or functional gas trapping because of conductive airway disease).

Although in an individual patient one of the two pathophysiologic conditions (ie, endotypes) may prevail, most patients with COPD present (phenotype) with a mixed disorder characterized by various combinations of both components, and a corresponding mixed CT subtype (4,5). Knowledge of the prevalent subtype in each patient may be of interest in developing clinical and pharmacological trials designed to target patient therapy to the underlying pathophysiologic mechanism of airflow obstruction. Conductive airway obstruction and parenchymal destruction may not be targetable with the same therapy. Therefore, our purpose was to identify a prevalent CT subtype in patients with COPD by separating emphysematous from nonemphysematous contributions to total gas trapping and to attempt to predict and grade the emphysematous gas trapping by using clinical and functional data.

Implications for Patient Care

- The definition of the prevalent CT subtype (ie, emphysema vs airway disease) of chronic obstructive pulmonary disease obtained by a coregistration method and by standard CT metrics could potentially be used to target patient therapy to the underlying chronic obstructive pulmonary disease endotype.
- A logistic model that combines body mass index and pulmonary function data can be used to predict CT-based quantification of emphysema grade, which may prove useful when assessing patients with chronic obstructive pulmonary disease who do not undergo thoracic CT.

Materials and Methods

This two-center study was approved by both institutional ethics committees of the University of Florence and the Catholic University of Sacred Heart in Rome. Written informed consent was obtained by all participants. The authors had control of the data and of the information submitted for publication.

Our study is a retrospective interpretation of prospectively acquired data. From January 2012 to December 2015, we recruited 224 consecutive eligible patients with COPD (Global Initiative for Chronic Obstructive Lung Disease stages I–IV) who met specific criteria: patients were aged 40–85 years, had a smoking history of more than 10 pack-years, showed nonreversible postbronchodilator airflow obstruction, and underwent chest CT within 48 hours of pulmonary function evaluation. We excluded patients who were within 1 month of an exacerbation or who had clinical conditions that interfered with pulmonary function or chest CT quantitative parameters assessment, including asthma, diffuse bronchiectasis, interstitial lung disease, acute heart failure, chemotherapy and/or radiation therapy, lung cancer, lung surgery, and metal objects in the chest.

Pulmonary Function Testing

Patients underwent complete pulmonary function evaluation within 48 hours of the CT examination. Pre- and postbronchodilator spirometry data, static lung volumes, and single-breath diffusing capacity for carbon monoxide were measured according to American Thoracic Society and European Respiratory Society guidelines (6).

Chest CT Images

Volumetric chest CT images were obtained at full inspiration and expiration by using the acquisition protocol adopted in the study by Regan et al (7). CT parameters were set as follows: 120 kVp; 200 mAs; rotation time, 0.5 seconds; pitch, 1.1; section thickness, 0.75 mm; and reconstructions kernels, b31f and b70f. All CT scans were performed by the same team of diagnostic personnel in each center (lead by F.B. and A.R.L., with 10 and 20 years of experience in thoracic imaging, respectively) and by using the same CT scanner for all patients in each center (Somatom Sensation 64, Siemens, Erlangen, Germany; and Somatom Definition Flash 128, Siemens). Patients were given instructions on how to perform the respiratory maneuvers

https://doi.org/10.1148/radiol.2017171519

Content code: CH

Radiology 2018; 287:683–692

Abbreviations:

COPD = chronic obstructive pulmonary disease

$\%LAA_{-950insp}$ = percentage lung attenuation area with CT attenuation values less than −950 HU at inspiration

$\%LAA_{-856exp}$ = percentage lung attenuation area with CT attenuation values less than −856 HU at expiration

Author contributions:

Guarantors of integrity of entire study, G.C., M. Pistolesi; study concepts/study design or data acquisition or data analysis/interpretation, all authors; manuscript drafting or manuscript revision for important intellectual content, all authors; approval of final version of submitted manuscript, all authors; agrees to ensure any questions related to the work are appropriately resolved, all authors; literature research, M.O., M. Paoletti, F.B., G.C., A.R.L., M. Pistolesi; clinical studies, F.B., G.C., R.I., A.R.L., M. Pistolesi; experimental studies, M.O., M. Paoletti, G.C., A.R.L.; statistical analysis, M.O., M. Paoletti, A.R.L.; and manuscript editing, all authors

Conflicts of interest are listed at the end of this article.

while lying supine in the CT scanner with arms fully abducted. No contrast medium was administered. Postprocessing image analysis was performed in images with reconstruction kernel b31f by a thoracic radiologist (M.O., with 5 years of experience in quantitative imaging). Thresholds at −950 HU and −856 HU were chosen as densitometric cut-off values consistent with emphysema and total gas trapping, respectively (8–10). The relative volumes of lung attenuation area with values below −950 HU at inspiration ($\%LAA_{-950insp}$) and below −856 HU at expiration ($\%LAA_{-856exp}$) were quantified by using a workstation for postprocessing image analysis of lung parenchyma and airways (Pulmonary Workstation Apollo 2.1; Vida Diagnostics, Coralville, Iowa). CT images were also analyzed by using another workstation for densitometric analysis of lung parenchyma (LDA; Imbio, Minneapolis, Minn), which is a U.S. Food and Drug–cleared and Conformité Européenne–mark certified medical device, which performs a deformable coregistration of paired inspiratory and expiratory CT scans, to obtain voxel-by-voxel attenuation maps. These maps, called pulmonary parametric response maps, classify lung voxels into three different tissue patterns on the basis of the attenuation values of each voxel: normal lung (percentage of voxels with CT attenuation greater than −950 HU at inspiration and greater than −856 HU at expiration), functional low density area (percentage of voxels with CT attenuation greater than −950 HU at inspiration and less than −856 HU at expiration), and persistent low density area (voxels with CT attenuation less than −950 HU at inspiration and less than −856 HU at expiration) (3). Moreover, pulmonary parametric response maps quantify the relative volumes of each lung pattern and show their regional distribution.

Data Analysis

Scatterplots were used to show the distribution and the relationships among CT parameters. Pearson *r* coefficient was used to assess association between parameters, and *P* values less than .05 indicated statistical significance.

To quantify the contribution of functional gas trapping to the CT reduced x-ray attenuation by using CT density thresholds without coregistration, we used the following computation:

$$\%fGT = \left[\%LAA_{-856\,exp} - \left(\%LAA_{-950insp} - 6\%\right)\right],$$

where *%fGT* is percentage of functional gas trapping, and 6% of voxels below −950 HU is assumed as the threshold value to diagnose emphysema at quantitative CT (1). To validate this computation we compared percentage of functional gas trapping with percentage of functional low density area.

To help separate the contribution of functional gas trapping from emphysema, the scatterplot of percentage of functional gas trapping and $\%LAA_{-950insp}$ of the whole series of patients was subdivided into four areas by drawing a line from the mean value of percentage of functional gas trapping on the x-axis (36.2%) and its perpendicular from the mean value of $\%LAA_{-950insp}$ on the y-axis (14.9%). Welch *t*, analysis of variance, and Games-Howell post hoc tests were used to evaluate differences of clinical and functional data between the four groups of patients entailed in each area (11).

The probability to have a $\%LAA_{-950insp}$ above or below the sample mean was estimated by a 10-fold validated logistic regression model built from stepwise selection of anthropometric, clinical, and functional data (Supplement E1 [online]) (12). A predicted probability value of the model output (*P*) of .5 was arbitrarily selected as decision threshold. For the sake of clinical classification, patients with a *P* value lower than .5 were subdivided in two subgroups according to a *P* value lower or higher than .2. Likewise, patients with a *P* value greater than .5 were subdivided in those with a *P* value greater or less than .8.

Data analysis and statistics were performed by using software (*S*-Plus 2000, Mathsoft, Cambridge, Mass; SPSS/PC Win 11.5.1, SPSS, Chicago, Ill; Mathcad version 2001, Mathsoft; and Microsoft Visual C++ 6.0, Microsoft, Redmond, Wash).

Table 1

Anthropometric, Pulmonary Function, and CT Metrics Data of 202 Patients with COPD

Parameter	Result
Age (y)	70.3 ± 8.1
BMI (kg/m²)	26.3 ± 4.6
Smoking history (pack-years)	50.8 ± 25.5
FEV_1 (%)	62.7 ± 26.3
FEV_1/VC (%)	47.1 ± 12.9
FEV_1/FVC (%)	51.4 ± 12.4
FVC (%)	92.8 ± 25.0
FRC (%)	128.6 ± 33.8
TLC (%)	107.7 ± 17.6
DLco (%)	68.5 ± 23.6
RV (%)	136.8 ± 48.3
RV/TLC (%)	50.2 ± 17.1
$LAA_{-950insp}$ (%)*	14.9 ± 12.4
$LAA_{-856exp}$ (%)*	45.1 ± 20.5
Normal lung (%)†	49.9 ± 21.1
fLDA (%)†	36.1 ± 14.0
pLDA (%)†	12.4 ± 12.7
fGT (%)	36.2 ± 13.6

Note.—Data are reported as mean ± standard deviation. BMI = body mass index, DLco = predicted diffusing capacity of lung for carbon monoxide, FEV_1 = forced expiratory volume in 1 second, fGT = functional gas trapping, fLDA = functional low density area, FRC = predicted functional residual capacity, FVC = predicted forced vital capacity, $LAA_{-950insp}$ = lung attenuation area with values below −950 HU at inspiratory CT scan, $LAA_{-856exp}$ = lung attenuation area with values below −856 HU at expiratory CT scan, pLDA = persistent low density area, RV = predicted residual volume, TLC = predicted total lung capacity, VC = vital capacity.

* Quantitative CT data calculated by Apollo 2.1 VIDA Software.

† Quantitative CT data calculated by LDA Imbio Software. Percentage of functional gas trapping is calculated as described in the Materials and Methods section.

Results

Of the 224 patients enrolled, 202 patients (159 men and 43 women; mean age, 71 years [age range, 41–85 years] and 67 years [age range, 46–84 years], respectively) were included in the analysis. Twenty-two patients were excluded for the presence of parenchymal consolidations (16 patients) or incomplete clinical (four patients) or CT scan (two patients) data. Anthropometric,

Table 2

Pearson Correlation Coefficients between Percentage of Functional Gas Trapping and Anthropometric, Smoking History, Pulmonary Function, and CT Imaging Data

	$\%LAA_{-950insp}$		pLDA%		$\%LAA_{-856exp}$		fLDA%		fGT%	
Parameter	*r* Value	*P* Value	*r* Value	*P* Value	*r* Value	*P* Value	*r* Value	*P* Value	*r* Value	*P* Value
Age	0.05		0.04		0.06		0.07		0.04	
BMI	−0.36	<.01	−0.37	<.01	−0.38	<.01	−0.22	<.01	−0.24	<.01
Pack-years	0.09		0.10		0.05		−0.02		−0.004	
FVC%	−0.17	<.05	−0.20	<.01	−0.26	<.01	−0.21	<.01	−0.23	<.01
FEV_1%	−0.48	<.01	−0.50	<.01	−0.58	<.01	−0.43	<.01	−0.44	<.01
FEV_1%/VC	−0.63	<.01	−0.64	<.01	−0.73	<.01	−0.52	<.01	−0.52	<.01
FEV_1%/FVC%	−0.66	<.01	−0.68	<.01	−0.72	<.01	−0.48	<.01	−0.48	<.01
TLC%	0.34	<.01	0.33	<.01	0.42	<.01	0.33	<.01	0.33	<.01
RV%	0.41	<.01	0.43	<.01	0.54	<.01	0.42	<.01	0.43	<.01
RV%/TLC%	0.35	<.01	0.37	<.01	0.42	<.01	0.31	<.01	0.31	<.01
FRC%	0.49	<.01	0.50	<.01	0.57	<.01	0.40	<.01	0.41	<.01
DLco%	−0.43	<.01	−0.45	<.01	−0.43	<.01	−0.24	<.01	−0.25	<.01
$\%LAA_{-950insp}$	1		0.99	<.01	0.76	<.01	0.26	<.01	0.24	<.01
$\%LAA_{-856exp}$	0.76	<.01	0.76	<.01	1		0.81	<.01	0.81	<.01
fLDA%	0.26	<.01	0.25	<.01	0.81	<.01	1		0.99	<.01
pLDA%	0.99	<.01	1		0.76	<.01	0.25	<.01	0.25	<.01
fGT%	0.24	<.01	0.25	<.01	0.81	<.01	0.99	<.01	1	

Note.—BMI = body mass index, DLco% = percentage of predicted diffusing capacity of lung for carbon monoxide, FEV_1% = percentage of predicted forced expiratory volume in 1 second, fGT% = percentage of functional gas trapping, fLDA% = percentage of functional low density area, FRC% = percentage of predicted functional residual capacity, FVC% = percentage of predicted forced vital capacity, $\%LAA_{-950insp}$ = percentage of lung attenuation area with values below −950 HU at inspiratory CT scan, $\%LAA_{-856exp}$ = percentage of lung attenuation area with values below −856 HU at expiratory CT scan, pLDA% = percentage of persistent low density area, RV% = percentage of predicted residual volume, TLC% = percentage of predicted total lung capacity, VC = vital capacity.

smoking history, lung function, and CT metrics data of the 202 patients are shown in Table 1.

Table 2 shows the correlations between clinical, pulmonary function, and CT data. The strongest correlations were observed between percentage of persistent low density area and $\%LAA_{-950insp}$, percentage of functional low density area and percentage of functional gas trapping, $\%LAA_{-856exp}$ and predicted forced expiratory volume in 1 second/vital capacity, and $\%LAA_{-856exp}$ and predicted forced expiratory volume in 1 second/forced vital capacity. Conversely, poor correlations were observed between CT metrics of functional gas trapping (ie, percentage of functional low density area and percentage of functional gas trapping) and functional and CT parameters compatible with emphysema (ie, percentage of diffusing capacity for carbon monoxide, predicted residual volume/predicted total lung capacity, and $\%LAA_{-950insp}$). CT metrics obtained by difference of density thresholds and those obtained by coregistration analysis correlated similarly with pulmonary function parameters.

Figure 1

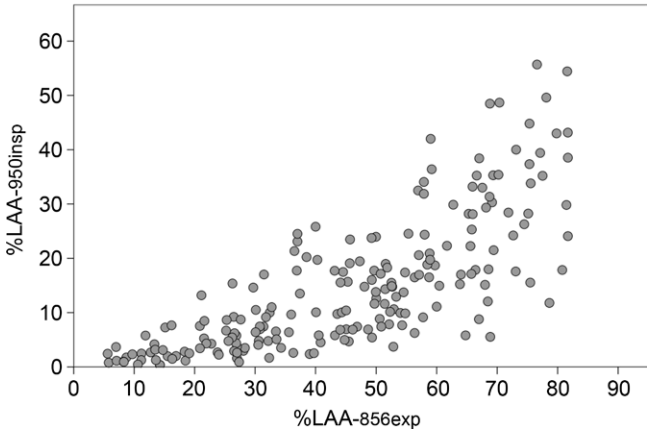

Figure 1: Scatterplot shows distribution of 202 patients with COPD according to CT imaging metrics of percentage of lung attenuation area with values below −950 HU at inspiratory CT scan *($\%LAA_{-950insp}$)* and percentage of lung attenuation area with values below-856HU at expiratory CT scan *($\%LAA_{-856exp}$)*. The two variables showed a substantial dispersion of data points that increased progressively with increasing severity of CT metrics changes. Patients with similar values of $\%LAA_{-950insp}$ had different values in $\%LAA_{-856exp}$.

Figure 1 shows the scatterplot of the 202 patients by using $\%LAA_{-950insp}$

Figure 2

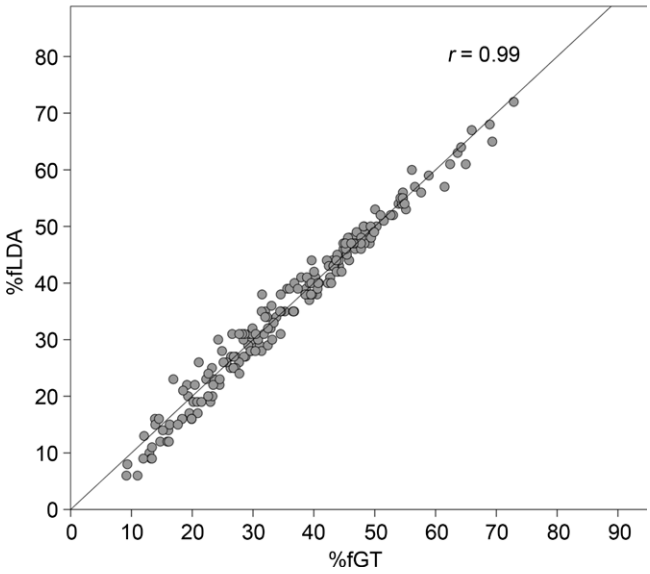

Figure 2: Scatterplot shows relationship between percentage of functional low density area *(%fLDA)* and percentage of functional gas trapping *(%fGT)*. The correlation between the two variables was strong, with a high Pearson *r* coefficient, and a regression line essentially corresponding to the identity line.

and $\%LAA_{-856exp}$ as coordinates. The dispersion of data points progressively increased with the increase in total gas trapping ($\%LAA_{-856exp}$), which indicated that there was a wide grade of interaction of emphysematous and nonemphysematous contribution to total gas trapping. In particular, patients with similar values of $\%LAA_{-950insp}$ had different values in $\%LAA_{-856exp}$. The nonemphysematous contribution to total gas trapping is a function of the difference of the two variables at each level $\%LAA_{-950insp}$, computed by percentage of functional gas trapping. Figure 2 shows the strong correlation between percentage of functional gas trapping and percentage of functional low density area, in which the regression line essentially corresponds to the identity line.

Figure 3 shows the relationship between the percentage of functional gas trapping (expression of functional gas trapping) and $\%LAA_{-950insp}$ (expression of emphysematous gas trapping). As can be derived from the graphical subgrouping of patients shown in Figure 3, the prevalent emphysema group (hereafter, referred to as the Emph group) consisted of 29 patients (14.4%) with prevalent emphysema ($\%LAA_{-950insp}$ higher than the mean value and percentage of functional gas trapping lower than the mean value), whereas prevalent functional gas trapping group (hereafter, referred to as the Funct group) consisted of 46 patients (22.8%) with prevalent functional (ie, nonemphysematous) gas trapping ($\%LAA_{-950insp}$ lower than the mean value and percentage of functional gas trapping higher than the mean value). There were 57 patients (28.2%) with a greater degree of severity of both components (hereafter, referred to as the Mixs group) and there were 70 patients (34.6%) who had a lower degree of severity of both components (hereafter, referred to as the Mixm group).

Table 3 shows the mean values of anthropometric, smoking history, and pulmonary function data across the four groups (Emph, Mixs, Mixm, and Funct in Fig 3). Body mass index was significantly higher in the Mixm group ($P < .01$), with a tendency to decrease as severity of disease increased. Percentage of diffusing capacity for carbon monoxide was the only parameter to differ significantly between the Emph and Funct groups ($P < .05$).

The logistic regression model was trained to classify patients with COPD according to the probability to have a $\%LAA_{-950insp}$ higher than the mean value of the sample. Predicted forced expiratory volume in 1 second/vital capacity, percent predicted forced expiratory volume in 1 second, percentage of diffusing capacity for carbon monoxide, and body mass index were included as predictors of $\%LAA_{-950insp}$, and four groups were defined according to the probability output. The overall accuracy of the probabilistic model was 81.1% in the training set and 79.2% in the validation set, with a higher accuracy (88.0%) in those patients with so-called milder disease (output model: $P < .5$) (Tables 4, 5). By combining functional indexes and body mass index predictors, we classified each patient according to probability output values ranging from milder (group 1) to more severe (group 4) emphysema. The four outputs of the model had significantly different $\%LAA_{-950insp}$ (or percentage of persistent low density area) ($P < .01$), as shown in Figure 4a. Figure 4b shows the relationship between percentage of functional low density area and total gas trapping ($\%LAA_{-856exp}$). The different colors on the scatterplot correspond to the four groups of emphysema grade estimated by the model on the basis of anthropometric and functional data. The regression line is fitted for data points with a model output less than 0.5 ($r = 0.89$). Patients with milder emphysema are distributed mainly along the regression line. Conversely, patients with a more severe parenchymal destruction are scattered above the regression line. The data point distribution reveals that in this series of patients with COPD, the emphysematous contribution to total gas trapping is absent for values of total gas trapping around or below 30%.

Discussion

Our study provides evidence that imaging metrics obtained by density thresholds difference of inspiratory and expiratory CT scans can be used to identify and quantify the relative contribution of functional (nonemphysematous) and emphysematous gas trapping and to identify a prevalent CT subtype. The evaluation of functional gas trapping obtained by density thresholds difference and coregistration analysis was comparable. The contribution of emphysema to total gas trapping, as assessed by CT, was estimated with reasonable accuracy by anthropometric and pulmonary function data.

Airflow obstruction in COPD results from both parenchymal destruction and small conducting airway disease, and small airway disease precedes the development of parenchymal destruction (13–15). Both pathophysiologic processes lead to gas trapping into the lungs. The differentiation of emphysematous gas trapping (because of parenchymal destruction) from functional gas trapping (because of conductive airway disease) is difficult both by pulmonary function testing and with CT scan (16,17). Recently, the pulmonary parametric response maps obtained through coregistration analysis of inspiratory and expiratory CT scan overcame this issue, allowing discrimination of the two contributions to total gas trapping (2,3,18).

We observed that the relationship between standard CT metrics ($\%LAA_{-950insp}$ and $\%LAA_{-856exp}$) was greatly dispersed, which suggested that total gas trapping ($\%LAA_{-856exp}$) included both emphysematous and nonemphysematous contributions. To determine these contributions we computed an index, called percentage of functional gas trapping, derived from the difference between standard CT metrics ($\%LAA_{-950insp}$ and $\%LAA_{-856exp}$) obtained from inspiratory and expiratory scans. The index had a strong correlation ($r = 0.99$) with percentage of functional low density area, which is the reference parameter for the nonemphysematous gas trapping derived by coregistration (2,3,18–20). Similar to percentage of functional low density area, percentage of functional gas trapping provides information on the amount of functional nonemphysematous gas trapping. In contrast to percentage of functional low density area, percentage of functional gas trapping lacks localization of gas trapping. Gas trapping regional distribution can be provided only by pulmonary parametric response maps, and may play a role in the assessment of symptoms severity and in the selection of patients for surgical and endoscopic lung volume reduction. However, percentage of functional gas trapping can be easily obtained by using widely available software programs on lung density analysis. This measurement can be supplemented by the qualitative evaluation of the regional distribution of the lung pathologic changes.

The weak correlation between CT metrics of parenchymal destruction ($\%LAA_{-950insp}$ and percentage of persistent low density area) and percentage of functional gas trapping depicted the independent contribution of functional gas trapping and parenchymal destruction to airflow obstruction. This was comparable to previous studies (5,21) that demonstrated weak correlations between indexes of emphysema severity and airway wall thickening.

The classification in four subgroups of patients (Emph, Mixs, Mixm, and Funct groups) to assess the relative contribution of functional gas trapping and parenchymal destruction in the definition of COPD subtypes was similar to that proposed in other studies

Figure 3

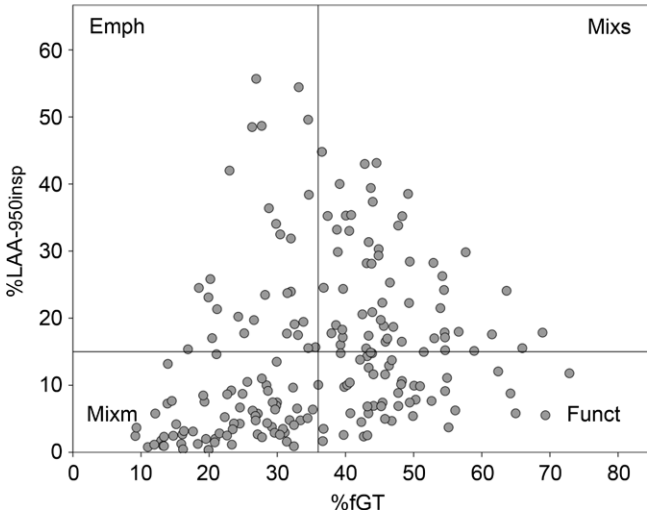

Figure 3: Scatterplot shows distribution of patients according to percentage of functional gas trapping *(%fGT)* and percentage of lung attenuation area with values below −950 HU at inspiratory CT scan *($\%LAA_{-950insp}$)*. The correlation between the two variables was weak ($r = 0.24$, $P < .01$). Lines representing mean values of $\%LAA_{-950insp}$ and percentage of functional gas trapping divide the scatterplot into four groups: prevalent emphysema (*Emph*; percentage of functional gas trapping lower than the mean value and $\%LAA_{-950insp}$ higher than the mean value), mixed-severe disease (*Mixs*; both percentage of functional gas trapping and $\%LAA_{-950insp}$ higher than the mean values), mixed-mild disease (*Mixm*; both percentage of functional gas trapping and $\%LAA_{-950insp}$ lower than the mean values), and prevalent functional gas trapping (*Funct*; percentage of functional gas trapping higher than the mean value and $\%LAA_{-950insp}$ lower than the mean value).

Table 3

Anthropometric, Smoking History, and Pulmonary Function Data among the Four Groups Derived by Contributions of Percentage of Functional Gas Trapping and $\%LAA_{-950insp}$ Parameters

Parameter	Emph Group	Mixs Group	Mixm Group	Funct Group	*P* Value
Age (y)	70.2	71.2	68.9	71.1	
BMI (kg/m^2)	25.1	24.4	28.6	25.9	
Emph vs Mixm	…	…	…	…	<.01
Mixs vs Mixm	…	…	…	…	<.01
Funct vs Mixm	…	…	…	…	<.01
Pack-years	56.3	52	48.6	49.1	NS
DLco%	55.2	59	81.4	67.3	
Emph vs Mixm	…	…	…	…	<.01
Mixs vs Mixm	…	…	…	…	<.01
Funct vs Mixm	…	…	…	…	<.01
Emph vs Funct	…	…	…	…	<.05
FVC%	97.9	87.5	98.6	87.3	
Mixs vs Mixm	…	…	…	…	<.05
Mixm vs Funct	…	…	…	…	<.05
FEV_1%	61.1	46.7	79.5	58.1	
Emph vs Mixs	…	…	…	…	<.05
Emph vs Mixm	…	…	…	…	<.01
Mixs vs Mixm	…	…	…	…	<.01
Funct vs Mixm	…	…	…	…	<.01
Mixs vs Funct	…	…	…	…	<.05
FEV_1/VC (%)	44.2	36.8	57.9	45.3	
Emph vs Mixs	…	…	…	…	<.05
Emph vs Mixm	…	…	…	…	<.05
Mixs vs Mixm	…	…	…	…	<.01
Mixs vs Funct	…	…	…	…	<.01
Mixm vs Funct	…	…	…	…	<.01
FEV_1/FVC (%)	48.4	40.8	61.3	51.1	
Emph vs Mixs	…	…	…	…	<.05
Emph vs Mixm	…	…	…	…	<.05
Mixs vs Mixm	…	…	…	…	<.01
Mixs vs Funct	…	…	…	…	<.01
Mixm vs Funct	…	…	…	…	<.01
TLC%	110.9	115.5	99.5	108.5	
Emph vs Mixm	…	…	…	…	<.05
Mixs vs Mixm	…	…	…	…	<.01
Mixm vs Funct	…	…	…	…	<.05
RV%	135.6	163	109.3	140.6	
Mixs vs Mixm	…	…	…	…	<.01
Mixs vs Funct	…	…	…	…	<.05
Mixm vs Funct	…	…	…	…	<.01
RV/TLC (%)	49.3	59.4	42.3	51.2	
Mixm vs Funct	…	…	…	…	<.01
Mixs vs Mixm	…	…	…	…	<.01
FRC%	131.9	150.3	109.2	129.2	
Emph vs Mixm	…	…	…	…	<.01
Mixs vs Mixm	…	…	…	…	<.01
Mixm vs Funct	…	…	…	…	<.01
Mixs vs Funct	…	…	…	…	<.01

Note.—Unless otherwise indicated, data are means. Differences between groups were analyzed by analysis of variance and Games-Howell posthoc tests. BMI = body mass index, DLco% = percentage of predicted diffusing capacity of lung for carbon monoxide, emph = group of patients with prevalent emphysema, FEV_1% = percentage predicted forced expiratory volume in 1 second, FRC% = percentage of predicted functional residual capacity, Funct = group of patients with prevalent functional gas trapping, FVC% = percentage of predicted forced vital capacity, Mixm = group of patients with lower degree of severity of emphysema and gas trapping, Mixs = group of patients with a greater degree of severity of both emphysema and functional gas trapping, NS = not significant, RV% = percentage of predicted residual volume, TLC% = percentage of predicted total lung capacity, VC = vital capacity.

* $P < .01$.

† $P < .05$

(14,21,22). Our patients displayed a continuous spectrum of pathologic alterations of both conductive airway disease and emphysema. However, knowledge of the percentage of lung destruction may be of help in assessing patient prognosis and, possibly, in selecting the individual treatment (eg, whether to add inhaled steroids to bronchodilators). Across the four subgroups of patients with COPD we observed no statistically significant differences in smoking history. Statistically significant higher diffusing capacity for carbon monoxide percentage values were found in patients in the Funct group versus in those in the Emph group. Patients in the Mixm group had significantly higher body mass index values than other subgroups. In agreement with previous studies (22,23), we found an inverse relationship between body mass index and CT indexes of emphysema, including $\%LAA_{-950insp}$ and percentage of persistent low density area. Accordingly, it is reasonable that body mass index was included among the regressors of the probabilistic model to predict the contribution of emphysema to total gas trapping. It was recently shown (24) that body mass index and height (the denominator in the body mass index formula) can be used to predict emphysema risk, with odds of emphysema increasing by 5% per 1-cm increase in body height.

Probabilistic models may help to characterize, without CT, the main pathophysiologic mechanism that underlies airflow obstruction and may facilitate individualized treatment strategies. This may be of relevance considering the high prevalence of COPD in the general population and the unavailability of CT imaging for most patients, even more so if we consider that both inspiratory and expiratory scans are needed. We found that body mass index combined in a predictive model with percentage of diffusing capacity for carbon monoxide predicted forced expiratory volume in 1 second and predicted forced expiratory volume in 1 second/vital capacity can be used to classify patients with

Table 4

Predictors and Odds Ratios of the Logistic Regression Model

Predictor	Odds Ratio	*P* Value
DLco%	0.98	.03
FEV_1/VC	0.87	<.01
BMI	3.41	<.01
FEV_1%	1.03	.02

Note.—The best regressors were selected after a stepwise procedure. The model classification cut-off was the predicted probability value of .5. BMI = body mass index, DLco% = percentage of predicted diffusing capacity of lung for carbon monoxide, FEV1% = percentage predicted forced expiratory volume in 1 second, *P* = predicted probability; VC = vital capacity.

Table 5

Accuracy of the Logistic Regression Model

Parameter	Class 1	Class 2	Accuracy (%)	Ten-fold Cross-validation Accuracy (%)
Class 1	103	14	88.0	88.0
Class 2	24	61	71.8	67.0
Overall accuracy			81.1	79.2

Note—Unless otherwise indicated, data are numbers of patients. Patients in class 1 included those with $P < .5$ (groups 1 and 2 in Fig 4) and patients in class 2 included those with $P > .5$ (groups 3 and 4 in Fig 4).

COPD according to CT parenchymal destruction ($\%LAA_{-950insp}$) with an acceptable level of accuracy. Previous studies (25,26) showed that parenchymal destruction on CT images is related to both percentage of diffusing capacity for carbon monoxide and predicted forced expiratory volume in 1 second, and that predicted forced expiratory volume in 1 second/vital capacity is better related to CT indexes ($\%LAA_{-950insp}$) of airway obstruction than predicted forced expiratory volume in 1 second/forced vital capacity. According to previous results, spirometric indexes of airflow obstruction had a moderate inverse correlation with emphysema indexes on CT images (27). These findings can be explained by the absence of a linear correlation between pulmonary function data and CT attenuation values, as demonstrated in a previous analysis (26).

The probabilistic index described here may help to differentiate, with acceptable approximation, the contribution of emphysema to total gas trapping in COPD. In patients with a predicted probability lower than 0.5 as output of the model, functional gas trapping approximately corresponded to total gas trapping. In patients with a predicted probability greater than 0.5 as output of the model, parenchymal destruction added to functional gas trapping increasing the overall value of total gas trapping ($\%LAA_{-856exp}$). This is comparable to the results obtained by McDonough et al (15), who by measuring mean linear intercept at micro-imaging showed that the narrowing and loss of terminal bronchioles preceded emphysematous destruction in COPD. In our patients, when total gas trapping was around or below 30%, it had no significant emphysematous contribution and was derived almost completely from the nonemphysematous component.

Our study had limitations. The main limitation of our study was the relatively small number of patients included in the cohort to be considered representative of the whole spectrum of COPD lung structural changes. Although our cohort was smaller than those of other studies (7,18), both the distribution and the mean of $\%LAA_{-950insp}$ and $\%LAA_{-856exp}$ obtained in our patients are comparable to those obtained in another study (7), which made the described model possibly suitable for application to other populations (28,29). Another limitation of this study was the use of the fixed ratio predicted forced expiratory volume in 1 second/forced vital capacity according to Global Initiative for Chronic Obstructive Lung Disease guidelines to enroll patients, instead of the use of age-dependent reference equations such as the lower limit of normality (30,31). The adoption of the fixed ratio may have over-diagnosed elderly patients who represented the vast majority of our population. Regarding CT, we lacked spirometric control of the level of lung inflation during the acquisition, and this may be an issue for reproducibility and data interpretation. However, patients were given careful instructions regarding how to perform the respiratory maneuvers while lying supine in the CT scanner. The presence of bronchiectasis and mucous impaction could have been another possible pitfall in the evaluation of lung density. However, none of our patients were studied during an exacerbation. Finally, the validation of the Logit model has been done on a training set (our cohort) and 10-fold cross-validated. It would be advisable to recruit a larger population in the near future, and to validate prospectively the model in a population different from that of the model derivation. A further limitation is the inclusion of only white patients, which may limit the application of the observed associations to other ethnicities.

In conclusion, our study demonstrated that standard imaging metrics obtained at inspiratory and expiratory thoracic CT scans can be used to identify and quantify the relative contribution of emphysematous and nonemphysematous gas trapping, permitting a better definition of COPD subtypes. Coregistration analysis adds information on regional distribution of disease type, extent, and severity, which cannot be provided by standard densitometric analyses. Furthermore, the use of a probabilistic model including anthropometric and functional data can grade the relative contribution of parenchymal destruction to total gas trapping as assessed by using CT. The application of this model may help to define different COPD subtypes and may be used to design newer outcomes in the development of clinical and pharmacologic trials.

Disclosures of Conflicts of Interest: M.O. Activities related to the present article: disclosed no relevant relationships. Activities not related to the present article: disclosed consultancies from Imbio. Other relationships: disclosed no relevant relationships. **M. Paoletti** disclosed no relevant relationships. **F.B.** disclosed no relevant relationships. **G.C.** disclosed no relevant relationships.

Figure 4

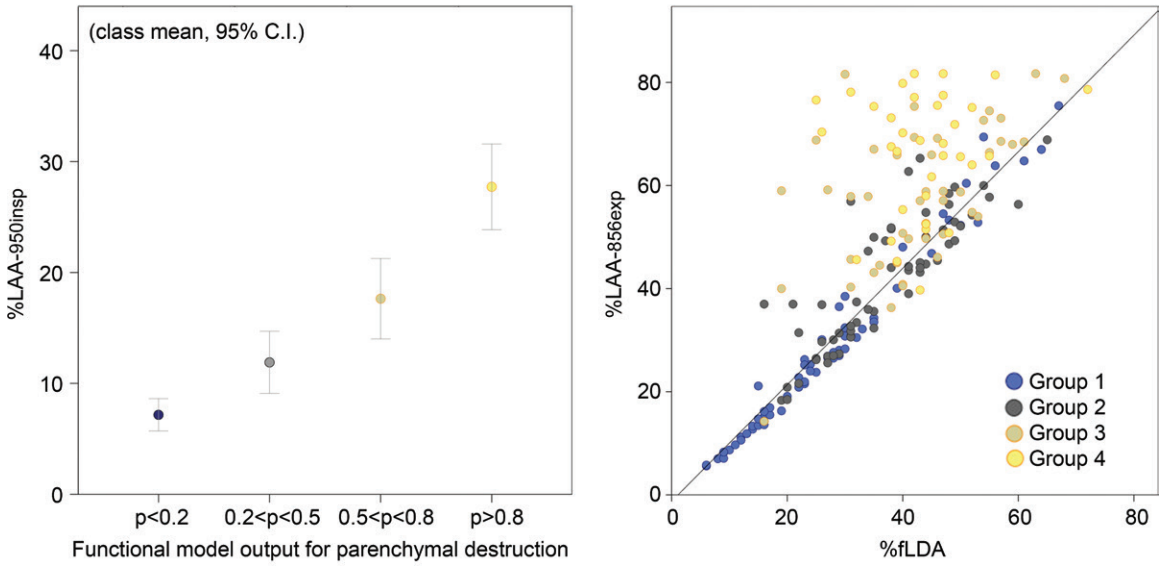

Figure 4: Output groups of the functional model and relationship between percentage of lung attenuation area with values below −856 HU at expiration *(%LAA$_{-856exp}$)* and percentage of functional low density area *(%fLDA)* across the output groups. **(a)** Modified box-and-whisker plot of mean values with corresponding 95% confidence intervals. The plot shows the distribution of percentage of lung attenuation area with values below −950HU at inspiration *(%LAA$_{-950insp}$)* across the four probability output groups of the logistic regression model. Group 1 ($n = 63$) represents a predicted probability output between 0 and 0.2, group 2 ($n = 61$) represents a predicted probability output between 0.2 and 0.5, group 3 ($n = 44$) represents a predicted probability output between 0.5 and 0.8, and group 4 ($n = 34$) represents a predicted probability output between 0.8 and 1. These groups have significantly different %LAA$_{-950insp}$ ($P < .01$). **(b)** Relationship between %LAA$_{-856exp}$ and percentage of functional low density area across the four output groups of the logistic regression model. Patients with milder emphysema (group 1) are distributed along the regression line ($r = 0.89$), whereas patients with more severe parenchymal destruction (groups 3 and 4) are scattered from this fitted line.

R.I. disclosed no relevant relationships. **A.R.L.** disclosed no relevant relationships. **M. Pistolesi** Activities related to the present article: disclosed no relevant relationships. Activities not related to the present article: personal fees and nonfinancial support from Glaxo-Smith-Kline; grants, personal fees, and nonfinancial support from Menarini; personal fees and nonfinancial support from Boehringer Iingelheim; personal fees and nonfinancial support from Astra Zeneca; personal fees and nonfinancial support from Chiesi; grants, personal fees, and nonfinancial support from Mundipharma; personal fees and nonfinancial support from Biofutura; grants, personal fees, and nonfinancial support from Novartis; personal fees and nonfinancial support from Guidotti Malesci; personal fees from Menarini International; grants from Sanofi; grants and personal fees from MSD; personal fees and nonfinancial support from Grifols; and grants from Bayer. Other relationships: disclosed no relevant relationships.

References

1. Lynch DA, Austin JH, Hogg JC, et al. CT-definable subtypes of chronic obstructive pulmonary disease: A Statement of the Fleischner Society. Radiology 2015;277(1):192–205.
2. Bhatt SP, Soler X, Wang X, et al. Association between functional small airway disease and FEV1 decline in chronic obstructive pulmonary disease. Am J Respir Crit Care Med 2016;194(2):178–184.
3. Galbán CJ, Han MK, Boes JL, et al. Computed tomography-based biomarker provides unique signature for diagnosis of COPD phenotypes and disease progression. Nat Med 2012;18(11):1711–1715.
4. Hogg JC. Pathophysiology of airflow limitation in chronic obstructive pulmonary disease. Lancet 2004;364(9435):709–721.
5. Camiciottoli G, Bigazzi F, Paoletti M, Cestelli L, Lavorini F, Pistolesi M. Pulmonary function and sputum characteristics predict computed tomography phenotype and severity of COPD. Eur Respir J 2013;42(3):626–635.
6. Miller MR, Hankinson J, Brusasco V, et al. Standardisation of spirometry. Eur Respir J 2005;26(2):319–338.
7. Regan EA, Hokanson JE, Murphy JR, et al. Genetic epidemiology of COPD (COPDGene) study design. COPD 2010;7(1):32–43.
8. Madani A, De Maertelaer V, Zanen J, Gevenois PA. Pulmonary emphysema: radiation dose and section thickness at multidetector CT quantification--comparison with macroscopic and microscopic morphometry. Radiology 2007;243(1):250–257.
9. Schroeder JD, McKenzie AS, Zach JA, et al. Relationships between airflow obstruction and quantitative CT measurements of emphysema, air trapping, and airways in subjects with and without chronic obstructive pulmonary disease. AJR Am J Roentgenol 2013;201(3):W460–W470.
10. Jain N, Covar RA, Gleason MC, Newell JD Jr, Gelfand EW, Spahn JD. Quantitative computed tomography detects peripheral airway disease in asthmatic children. Pediatr Pulmonol 2005;40(3):211–218.
11. Olejnik S, Li J, Supattathum S, Huberty CJ. Multiple testing and statistical power with

modified Bonferroni procedures. J Educ Behav Stat 1997;22(4):389–406.

12. Hilbe JM. Logistic regression models. Boca Raton, Fla: CRC, 2009.
13. Gelb AF, Schein M, Kuei J, et al. Limited contribution of emphysema in advanced chronic obstructive pulmonary disease. Am Rev Respir Dis 1993;147(5):1157–1161.
14. Nakano Y, Müller NL, King GG, et al. Quantitative assessment of airway remodeling using high-resolution CT. Chest 2002;122(6 Suppl):271S–275S.
15. McDonough JE, Yuan R, Suzuki M, et al. Small-airway obstruction and emphysema in chronic obstructive pulmonary disease. N Engl J Med 2011;365(17):1567–1575.
16. Camiciottoli G, Bartolucci M, Maluccio NM, et al. Spirometrically gated high-resolution CT findings in COPD: lung attenuation vs lung function and dyspnea severity. Chest 2006;129(3):558–564.
17. Han MK. Clinical correlations of computed tomography imaging in chronic obstructive pulmonary disease. Ann Am Thorac Soc 2013;10(Suppl):S131–S137.
18. Martinez CH, Diaz AA, Meldrum C, et al. Age and small airway imaging abnormalities in subjects with and without airflow obstruction in SPIROMICS. Am J Respir Crit Care Med 2017;195(4):464–472.
19. Capaldi DP, Zha N, Guo F, et al. Pulmonary imaging biomarkers of gas trapping and emphysema in COPD: (3)He MR Imaging and CT parametric response maps. Radiology 2016;279(2):597–608.
20. Pompe E, van Rikxoort EM, Schmidt M, et al. Parametric response mapping adds value to current computed tomography biomarkers in diagnosing chronic obstructive pulmonary disease. Am J Respir Crit Care Med 2015;191(9):1084–1086.
21. Subramanian DR, Gupta S, Burggraf D, et al. Emphysema- and airway-dominant COPD phenotypes defined by standardised quantitative computed tomography. Eur Respir J 2016;48(1):92–103.
22. Ogawa E, Nakano Y, Ohara T, et al. Body mass index in male patients with COPD: correlation with low attenuation areas on CT. Thorax 2009;64(1):20–25.
23. Lee YK, Oh YM, Lee JH, et al. Quantitative assessment of emphysema, air trapping, and airway thickening on computed tomography. Lung 2008;186(3):157–165 [Published correction appears in Lung 2008; 186(4):277.].
24. Miniati M, Bottai M, Pavlickova I, Monti S. Body height as risk factor for emphysema in COPD. Sci Rep 2016;6(1):36896.
25. Desai SR, Hansell DM, Walker A, MacDonald SL, Chabat F, Wells AU. Quantification of emphysema: a composite physiologic index derived from CT estimation of disease extent. Eur Radiol 2007;17(4):911–918.
26. Paoletti M, Cestelli L, Bigazzi F, Camiciottoli G, Pistolesi M. Chronic obstructive pulmonary disease: pulmonary function and CT lung attenuation do not show linear correlation. Radiology 2015;276(2):571–578.
27. Nakano Y, Muro S, Sakai H, et al. Computed tomographic measurements of airway dimensions and emphysema in smokers. Correlation with lung function. Am J Respir Crit Care Med 2000;162(3 Pt 1):1102–1108.
28. Lynch DA, Al-Qaisi MA. Quantitative computed tomography in chronic obstructive pulmonary disease. J Thorac Imaging 2013; 28(5):284–290.
29. Nambu A, Zach J, Schroeder J, et al. Quantitative computed tomography measurements to evaluate airway disease in chronic obstructive pulmonary disease: Relationship to physiological measurements, clinical index and visual assessment of airway disease. Eur J Radiol 2016;85(11):2144–2151.
30. Brusasco V. Spirometric definition of COPD: exercise in futility or factual debate? Thorax 2012;67(7):569–570.
31. Luoto JA, Elmståhl S, Wollmer P, Pihlsgård M. Incidence of airflow limitation in subjects 65-100 years of age. Eur Respir J 2016;47(2):461–472.